

Synapse

Copy of e-mail Notification

Synapse Published by John Wiley & Sons, Inc.

Dear Author,

Your article page proof for Synapse is ready for your final content correction within our rapid production workflow. The PDF file found at the URL given below is generated to provide you with a proof of the content of your manuscript. Once you have submitted your corrections, the production office will proceed with the publication of your article.

John Wiley & Sons has made this article available to you online for faster, more efficient editing. Please follow the instructions below and you will be able to access a PDF version of your article as well as relevant accompanying paperwork.

First, make sure you have a copy of Adobe Acrobat Reader software to read these files. This is free software and is available for user downloading at <http://www.adobe.com/products/acrobat/readstep.html>.

Open your web browser, and enter the following web address:

<http://cps.kwglob.com/jw/retrieval.aspx?pwd=165d2258761b>

You will be prompted to log in, and asked for a password. Your login name will be your email address, and your password will be 165d2258761b

Example:

Login: your e-mail address

Password: 165d2258761b

The site contains one file, containing:

- Author Instructions Checklist
- Annotated PDF Instructions
- Reprint Order Information
- A copy of your page proofs for your article

In order to speed the proofing process, we strongly encourage authors to correct proofs by annotating PDF files. Any corrections should be returned to SYNprod@wiley.com 1 to 2 business days after receipt of this email in order to achieve our goal of publishing your article online 15 days from the day final data was received.

Please see the Instructions on the Annotation of PDF files included with your page proofs. Please take care to

Synapse

Copy of e-mail Notification

answer all queries on the last page of the PDF proof; proofread any tables and equations carefully; and check that any Greek characters (especially "mu") have converted correctly. Please check your figure legends carefully.

- answer all queries on the last page of the PDF proof
- proofread any tables and equations carefully
- check your figure(s) and legends for accuracy

Within 1 to 2 business days, please return page proofs with corrections and any relevant forms to:

Production Editor, SYN

E-mail: SYNprod@wiley.com

Technical problems? If you experience technical problems downloading your file or any other problem with the website listed above, please contact Balaji (e-mail: Wiley.CS@cenveo.com, phone: +91 (44) 4205-8810 (ext.308)). Be sure to include your article number.

Questions regarding your article? Please don't hesitate to contact me with any questions about the article itself, or if you have trouble interpreting any of the questions listed at the end of your file. **REMEMBER TO INCLUDE YOUR ARTICLE NO. (21984) WITH ALL CORRESPONDENCE.** This will help us address your query most efficiently.

As this e-proofing system was designed to make the publishing process easier for everyone, we welcome any and all feedback. Thanks for participating in our e-proofing system!

This e-proof is to be used only for the purpose of returning corrections to the publisher.

Sincerely,

Production Editor, SYN

E-mail: SYNprod@wiley.com



111 RIVER STREET, HOBOKEN, NJ 07030

*****IMMEDIATE RESPONSE REQUIRED*****

Your article will be published online via Wiley's EarlyView® service (wileyonlinelibrary.com) shortly after receipt of corrections. EarlyView® is Wiley's online publication of individual articles in full text HTML and/or pdf format before release of the compiled published issue of the journal. Articles posted online in EarlyView® are peer-reviewed, copyedited, author corrected, and fully citable via the article DOI (for further information, visit www.doi.org). EarlyView® means you benefit from the best of two worlds--fast online availability as well as traditional, issue-based archiving.

Please follow these instructions to avoid delay of publication.

☐ **READ PROOFS CAREFULLY**

- This will be your only chance to review these proofs. **Please note that once your corrected article is posted online, it is considered legally published, and cannot be removed from the Web site for further corrections.**
- Please note that the volume and page numbers shown on the proofs are for position only.

☐ **ANSWER ALL QUERIES ON PROOFS** (If there are queries they will be found on the last page of the PDF file.)

- In order to speed the proofing process, we strongly encourage authors to correct proofs by annotating PDF files. Please see the instructions on the Annotation of PDF files. If unable to annotate the PDF file, please print out and mark changes directly on the page proofs.

☐ **CHECK FIGURES AND TABLES CAREFULLY**

- Check size, numbering, and orientation of figures.
- All images in the PDF are downsampled (reduced to lower resolution and file size) to facilitate Internet delivery. These images will appear at higher resolution and sharpness in the final, published article.
- Review figure legends to ensure that they are complete.
- Check all tables. Review layout, title, and footnotes.

RETURN

☐ **PROOFS**

☐ **Other forms, as needed**

Return corrections immediately via email to SYNprod@wiley.com


QUESTIONS

Production Editor, SYN

E-mail: SYNprod@wiley.com

Refer to journal acronym and article production number
(i.e., SYN 00-0000 for SYNAPSE ms 00-0000).

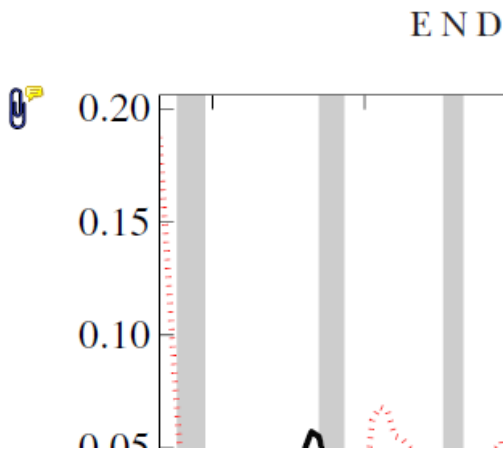
5. **Attach File** Tool – for inserting large amounts of text or replacement figures.



Inserts an icon linking to the attached file in the appropriate place in the text.

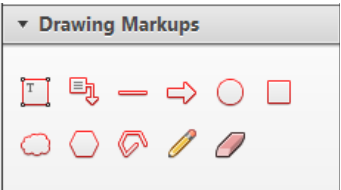
How to use it

- Click on the **Attach File** icon in the Annotations section.
- Click on the proof to where you'd like the attached file to be linked.
- Select the file to be attached from your computer or network.
- Select the colour and type of icon that will appear in the proof. Click OK.



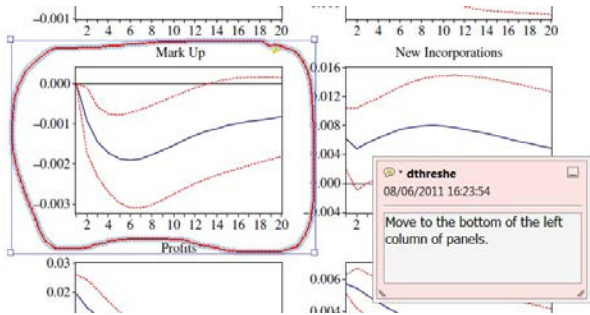
6. **Drawing Markups** Tools – for drawing shapes, lines and freeform annotations on proofs and commenting on these marks.

Allows shapes, lines and freeform annotations to be drawn on proofs and for comment to be made on these marks.



How to use it

- Click on one of the shapes in the Drawing Markups section.
- Click on the proof at the relevant point and draw the selected shape with the cursor.
- To add a comment to the drawn shape, move the cursor over the shape until an arrowhead appears.
- Double click on the shape and type any text in the red box that appears.





Additional reprint purchases

Should you wish to purchase additional copies of your article, please click on the link and follow the instructions provided:

<https://caesar.sheridan.com/reprints/redir.php?pub=10089&acro=SYN>

Corresponding authors are invited to inform their co-authors of the reprint options available.


Please note that regardless of the form in which they are acquired, reprints should not be resold, nor further disseminated in electronic form, nor deployed in part or in whole in any marketing, promotional or educational contexts without authorization from Wiley. Permissions requests should be directed to mail to: permissionsus@wiley.com

For information about 'Pay-Per-View and Article Select' click on the following link: wileyonlinelibrary.com/aboutus/ppv-articleselect.html

RESEARCH ARTICLE

WILEY **SYNAPSE**

Interleukin 6 trans-signaling regulates basal synaptic transmission and sensitivity to pentylenetetrazole-induced seizures in mice

Roberto Cuevas-Olguin^{1*} | Eric Esquivel-Rendon^{1*} | Jorge Vargas-Mireles¹ |
 Francisco Garcias-Oscos² | Marcela Miranda-Morales¹ | Humberto Salgado³ |
 Stefan Rose-John⁴ | Marco Atzori^{1,5} 

¹Faculty of Science, Universidad Autónoma de San Luis Potosí, Av. Salvador Nava S/N, San Luis Potosí, San Luis Potosí 78290, México

²Department of Psychiatry, Southwestern University, 5323 Harry Hines Boulevard, Dallas, Texas 75390

³Centro de Investigaciones Regionales Hideyo Noguchi, Universidad Autónoma de Yucatán, Calle 60 491-A, Centro, Mérida, YUC 97000, México

⁴Department of Biochemistry, Christian Albrecht Universität, Christian-Albrechts-Platz 4, Kiel 24118, Germany

⁵School of Behavioral and Brain Sciences, University of Texas, 800 West Campbell Road, Richardson, Dallas, Texas 75080

Correspondence

Marco Atzori, Universidad Autonoma de San Luis Potosí, Programa de Biología, Facultad de Ciencias, Edificio 1, Avenida Salvador Nava s/n, San Luis Potosi, SLP 78290, México

Email: marco.atzori@uaslp.mx or

marco_atzori@hotmail.com

Funding information

The work has been conducted with funds from CONACyT (CB-2013-01 221653) and PROMEP 2014 to M.A.

Abstract

The pro-inflammatory cytokine interleukin 6 (IL-6) interacts with the central nervous system in a largely unknown manner. We used a genetically modified mouse strain (GFAP-sgp130Fc, TG) and wild type (WT) mice to determine whether IL-6 trans-signaling contributes to basal properties of synaptic transmission. Postsynaptic currents (PSCs) were studied by patch-clamp recording in cortical layer 5 of a mouse prefrontal cortex brain slice preparation. TG and WT animals displayed differences mainly (but not exclusively) in excitatory synaptic responses. The frequency of both action potential-independent (miniature) and action potential-dependent (spontaneous) excitatory PSCs (ePSCs) were higher for TG vs. WT animals. No differences were observed in inhibitory miniature, spontaneous, or tonic inhibitory currents. The pair pulse ratio (PPR) of electrically evoked inhibitory as well as of excitatory PSCs were also larger in TG animals vs. WT ones, while no changes were detected in electrically evoked excitatory-inhibitory synaptic ratio (eEPSC/eIPSC), nor in the ratio between the amino-propionic acid receptor (AMPA)-mediated and N-methyl D aspartate-R (NMDAR)-mediated components of eEPSCs (I_{AMPA}/I_{NMDA}). Evoked IPSC rise times were shorter for TG vs. WT animals. We also compared the sensitivity of TG and WT animals to pentylenetetrazole (PTZ)-induced seizures. We found that TG animals were more sensitive to PTZ injections, as they displayed longer and more severe seizures. We conclude that the absence of basal IL-6 trans-signaling contributes to increase the basal excitability of the central nervous system, at the system level as well at the synaptic level, at least in the prefrontal cortex.

KEYWORDS

GABA, glutamate, interleukin 6, mice, patch-clamp, pentylenetetrazole, prefrontal cortex, seizures, synaptic transmission, trans-signaling

1 | INTRODUCTION

Interleukin-6 (IL-6) is a pro-inflammatory cytokine that has been involved in the etiology of a family of neuropsychiatric conditions including depression (Monje et al., 2011; Sukoff Rizzo et al., 2012), schizophrenic psychoses (Behrens, Ali, & Dugan, 2008), anxiety disorders

(Belem da Silva et al., 2016), and epilepsy (Lehtimäki, Liimatainen, Peltola, & Arvio, 2011; Li et al., 2011). It has been proposed that IL-6 alters central nervous system (CNS) excitability by modifying synaptic transmission in stress-sensitive brain areas (Atzori, Garcia-Oscos, & Mendez, 2012), and that *trans-signaling* is the main mechanism of action of IL-6 in the brain (Campbell et al., 1993, 2014).

IL-6 carries out its function through two pathways, both leading to activation of the janus kinase/activator of transcription JAK/STAT: a "classic" pathway, associated with the one-step activation of a

*Roberto Cuevas-Olguin and Eric Esquivel-Rendon contributed equally to this study.

multimeric complex constituted by the IL-6 receptor (IL-6 R) and the transducer protein glycoprotein 130 (gp130), present in immune cells and hepatocytes, as well as a second pathway, denominated “*trans-signaling*”, a multistep process consisting in binding of IL-6 to soluble IL-6 R molecules shed by immune cells and glia, followed by binding of the IL-6/IL-6 R complex to gp130, pathway that is available to all nucleated cells (Rose-John, 2012; Waetzig & Rose-John, 2012; Wolf, Rose-John, & Garbers, 2014). The importance of the second pathway has been underscored in the CNS through the use of a genetically modified mouse strain (GFAP-sgp130Fc, TG) in which a construct for a soluble version of the gp130 (sgp130Fc) has been introduced in the promoter for the glial fibrillary acidic protein (GFAP), an astrocyte marker (Chalaris, Garbers, Rabe, Rose-John, & Scheller, 2011; Nowell et al., 2009). Previous work has shown that this genetic modification greatly impairs the effects of IL-6 in the CNS, presumably by sequestration of IL-6/IL-6 R complexes from the cerebro-spinal fluid (CSF) (Campbell et al., 2014). In fact, TG mice display altered sleep (Benedict, Scheller, Rose-John, Born, & Marshall, 2009; Oyanedel, Kelemen, Scheller, Born, & Rose-John, 2015) and altered anesthesia sensitivity (Braun et al., 2013), suggesting that most central effects of IL-6 within the brain are mediated by *trans-signaling* rather than by the “*classic*” signaling (Campbell et al., 2014).

In particular, we and others have found that IL-6 acutely and transiently impairs inhibitory γ -amino butyric acid (GABA)-ergic signaling in the CNS (Garcia-Oscos et al., 2012; Kawasaki, Zhang, Cheng, & Ji, 2008), and that sgp130Fc mice display a differential sensitivity of GABAergic synapses in response to lipopolysaccharide (LPS) systemic challenge (Garcia-Oscos et al., 2015). In the latter work we showed that maximal electrically evoked inhibitory currents in GFAP-sgp130Fc mice are higher than those of WT animals, suggesting that basal inhibitory—and possibly excitatory—transmission may be affected by IL-6 *trans-signaling*.

An important open question is whether IL-6 *trans-signaling* plays any role in the development and establishment of neocortical synapses and its properties. We tackled the problem by systematically comparing synaptic transmission in basal conditions between wild-type (WT) and TG mice, using patch-clamp recording in a prefrontal cortical slice preparation. We detected several differences both in inhibitory and in excitatory synaptic transmission. In order to test the overall systemic effect of IL-6 *trans-signaling* on brain excitability we also compared the seizure sensitivity to the convulsive agent pentylenetetrazole (PTZ) for TG vs. WT animals, finding that TG animals are more sensitive than WT to PTZ.

2 | MATERIALS AND METHODS

2.1 | Preparation

For this study we used 43 WT mice (C57BL/6 J, Charles River, 22 male, 21 female) and other 45 mice of the same strain, offspring from mice genetically modified in the laboratory of SRJ (GFAP-sgp130Fc, or TG, 24 male, 21 female), in the age range between 2 and 3 month-old (average age 73 ± 15 d/o).

2.2 | GFAP-sgp130Fc mice

A vector containing the human glial fibrillary acidic protein GFAP promoter cloned upstream of the optimized soluble glycoprotein 130Fc (sgp130Fc) (Campbell et al., 2014; Rabe et al., 2008) was used for the construction of the transgenic mice expressing sgp130Fc in the central nervous system by astrocytes (GFAP-sgp130Fc mice); a Bcl II/Not I fragment of 5854 bp was isolated from the plasmid and injected into oocytes, which were implanted into foster mothers. The following primers were used for genotyping sgp130Fc mice: sgp130-Fc-screen forward: 5'-GAG TTC AGA TCC TGC GAC-3' sgp130-Fc-screen reverse: 5'-TCA CTT GCC AGG AGA CAG-3'

2.3 | Brain slices

We chose to analyze the synaptic properties of the medial prefrontal cortex, an area that has long been implicated in the etiology and expression of neurologic and psychiatric disease (Holmes & Wellman, 2009). Mice were anesthetized with isoflurane and sacrificed according to the Norma Nacional Mexicana (UASLP protocol n. 2240) and their brains sliced with a vibrotome (VT1000, Leica) in a cold solution (0–4°C) containing (mM) 126 NaCl, 3.5 KCl, 10 glucose, 25 NaHCO₃, 1.25 NaH₂PO₄, 1.5 CaCl₂, 1.5 MgCl₂, at pH 7.4, and saturated with a mixture of 95% O₂ and 5% CO₂ (ACSF). Coronal slices (270 μ m thick) were taken from the medial prefrontal cortex and incubated in ACSF at 32°C before being placed in the recording chamber.

2.4 | Drugs

Different extracellular solutions were used for different electrophysiology experiments. Pharmacologically isolated inhibitory currents were recorded using a solution containing 6,7-dinitroquinoxaline-2, 3-dione (10 μ M) and kynurenate (2 mM) for blocking α -amino-3-hydroxy-5-methyl-4-isoxazolepropionic acid receptor (AMPA)- and N-methyl-D-aspartate receptor (NMDAR)-mediated currents, respectively. Pharmacologically isolated glutamatergic currents were recorded in the presence of the GABA_AR blocker picrotoxin (100 μ M) or bicuculline methiodide (10 μ M). Tetrodotoxin was dissolved in a 1 mM stock aqueous solution and bath-applied at a final concentration of 1 μ M for blocking action potentials. Pentylenetetrazole (PTZ) was also prepared in aqueous solution and administered via i.p. injections at the doses indicated in the text. All drugs were purchased from Sigma (St. Louis, MP) or Tocris (Ellisville, MO).

2.5 | Electrophysiology

2.5.1 | General

Slices were placed in an immersion chamber, and cells were selected using procedures described previously (Roychowdhury et al., 2014) using an upright microscope (BX51, Olympus) with a 60X objective and an infrared camera system (DAGE-MTI, Michigan City, IN). Whole-cell voltage-clamp recordings were obtained from cortical L5 pyramidal neurons of the mPFC. Neurons were selected by their pyramidal shape and pronounced apical dendrite, indicative of their pyramidal cell

nature (Atzori, Kanold, Pineda, Flores-Hernandez, & Paz, 2005). A 5-mV voltage step was applied at the beginning of every episode in order to monitor the quality of the recording. Access resistance (10–20 M Ω) was monitored throughout the experiment. Recordings with >20% change in input resistance (R_m) was discarded from the analysis. All signals were filtered at 2 kHz and sampled at 10 kHz. All experiments were performed at room temperature (22–23°C).

2.5.2 | Miniature and spontaneous PSCs

Recordings of inhibitory or excitatory postsynaptic currents (PSCs) were performed in the whole-cell configuration, in voltage-clamp mode, at a holding membrane potential of $V_h = -60$ mV, with 3–5 M Ω electrodes filled with a solution containing (mM) 100 CsCl, 5 1,2-bis(2-aminophenoxy)-ethane-*N,N,N',N'*-tetraacetic acid K (BAPTA-K), 1 lidocaine *N*-ethyl bromide (QX314), 1 MgCl₂, 10 *N*-(2-hydroxyethyl) piperazine-*N'*-(2-ethanesulfonic acid), 4 glutathione, 3 ATPMg₂, 0.3 GTPNa₂, and 20 phosphocreatine. The holding voltage was not corrected for the junction potential (< 4 mV). The intracellular recording solution was titrated to pH 7.35 and had an osmolarity of 267 ± 3 mOsm. Miniature IPSCs (mIPSCs) were recorded in the presence of the Na⁺ channel blocker tetrodotoxin (TTX, 1 μ M).

2.5.3 | Tonic GABAergic currents

Extrasynaptic GABA_AR are characterized by the presence of a specific subunit—denominated δ subunit (Drasbek & Jensen, 2006). We used 4,5,6,7-tetrahydroisoxazolo(5,4-*c*)pyridin-3-ol (THIP, or gaboxadol) to specifically enhance δ subunit-mediated extrasynaptic GABA_AR-mediated extrasynaptic currents, which we estimated by determining the picrotoxin-induced change in holding current (I_h) following previous bath-application of gaboxadol (5 μ M). After recording an initial baseline, THIP was first bath-applied for 10 minutes or longer, until it yielded a stable condition, after which picrotoxin (100 μ M) was applied on top of THIP, in order to determine the tonic GABA_AR-dependent component of the holding current (I_h) (Banerjee et al., 2013; Drasbek & Jensen, 2006). For I_h normalization we calculated neuronal surface area as proportional to the capacitance, calculated from the decay time of a 5 mV pulse delivered at every acquisition sweep.

2.5.4 | Electrically evoked synaptic currents

Evoked excitatory and inhibitory PSCs (eEPSC and eIPSCs) were measured by delivering two electric stimuli (≤ 200 μ s, 0–100 μ A) 200 ms apart every 12 s with an isolation unit (A360 WPI, Sarasota FL), through a glass stimulation pipette using a monopolar electrode filled with ACSF and placed at 150–200 μ m away from the recording electrode with an isolation unit, through a glass stimulation monopolar electrode filled with ACSF. The responses were monitored at different stimulation intensities prior to baseline recording.

2.5.4.1 | Excitatory-inhibitory synaptic ratio

In order to determine inhibitory and excitatory currents within a single cell we used a low-Cl[−] containing intracellular solution where CsCl was lowered to 10 mM, and the remainder 90 mM was substituted with K⁺ gluconate, resulting in a theoretical reversal potential for Cl[−] of approxi-

mately −65 mV, similar to a procedure previously described (Garcia-Oscos et al., 2012). The holding voltage was corrected for the junction potential ($V_{\text{offset}} \approx 9$ mV). The intracellular recording solutions were titrated to pH 7.3 and had an osmolarity of approximately 270 mOsm.

Reversal potential for postsynaptic currents were evaluated determining current–voltage (*I*–*V*) relationships for the evoked postsynaptic current (peak amplitude of 10 events at each holding potential V_h in the range from $V_h = -90$ mV up to $V_h = +60$ mV). Evoked IPSCs reversed polarity close to the theoretical reversal potential of −65 mV (-64 ± 2 mV, $n = 3$), while evoked EPSCs reversed at $V_{\text{exc}} = 10.5 \pm 3$ mV ($n = 3$).

2.5.4.2 | AMPAR- vs. NMDAR-mediated ratio

We also used patch-clamp recording for measuring the ratio between *N*-methyl-D-aspartate-receptor-mediated currents (I_{NMDA}) and α -amino-3-hydroxy-5-methyl-4-isoxazolepropionic-acid-receptor-mediated currents (I_{AMPA}), similar to previous work (Dufour, Liu, Gusev, Alkon, & Atzori, 2006). Briefly, the control solution contained bicuculline methachloride (10 μ M) for blocking GABA_AR-mediated currents. Postsynaptic currents were recorded with 3–5 M Ω electrodes using a solution containing the following (in mM): 100 CsOH, 100 gluconic acid, 5 1,2-bis(2-aminophenoxy)ethane-*N,N,N',N'*-tetraacetic acid K (BAPTA-K), 1 lidocaine *N*-ethyl bromide (QX314), 1 MgCl₂, 10 *N*-(2-hydroxyethyl)piperazine-*N'*-(2-ethanesulfonic acid) (HEPES), 4 glutathione, 1.5 ATPMg₂, 0.3 GTPNa₂. Electrically evoked EPSC were measured by delivering two electric stimuli (200 μ s, 10–50 μ A). I_{AMPA} were recorded at a holding potential $V_r = -60$ mV and measured at their peak. I_{NMDA} were recorded in the same cell at $V_r = +60$ mV in order to remove the Mg²⁺ block at NMDA receptors. I_{NMDA} amplitude measured at a latency of 45 ms after the electric stimulation for minimizing the possible contamination by I_{AMPA} . The stability of the recording was assessed by measuring I_{AMPA} both prior and subsequent to the measurement of I_{NMDA} . Only recordings in which I_{AMPA} measured before and after I_{NMDA} differed by < 20% were considered.

2.6. | PTZ-evoked seizures

2.6.1 | Assessment of the optimal convulsive dose

We prepared Pentylentetrazole (Sigma) at a concentration of 2.5 mg/ml in saline buffer (NaCl 0.9%). A pilot test was performed to determine the concentration to use, testing concentrations in ascending order 25, 50, 75, and 100 mg/kg, injected intraperitoneally into mice of the C57BL/6 strain ($n = 3$ each dose). No effects were observed at 25 mg/kg, while at 50 mg/kg all three animals showed and survived an epileptic event, and all animals injected with a dose ≥ 75 mg/kg died following the seizure. To assess the severity of convulsions we used a standard Racine test, consisting in the following scale: stage 0—normal behavior; stage 1—hypoactivity, immobility; stage 2—rigidity, whisker twitching; stage 3—reared, rigid posture, some automatisms (e.g., forelimb pawing, head bobbing, tail whipping); stage 4—intermittent rearing and falling with forelimb/jaw clonus, stage 5—continuous rearing and falling > 30 s or continuous jumping (popcorning); stage 6—generalized tonic-clonic seizures with whole body convulsions (Getova &

Mihaylova, 2011). For each 5-minute interval the highest seizure stage reached was recorded. We quantified the effects of the PTZ i.p. injections of 40, 50, and 60 mg/kg in terms seizure *latency* (defined as the duration of the interval between the PTZ injection and the behavioral entry to stage 1), *start* (time interval between PTZ injection and the actual seizure onset), number of turns, and *duration* of the event ($n = 3$). None of the parameters significantly differed for different concentrations, except for the event *latency*, which was substantially shorter for 50 mg/kg compared to lower doses, presented a small variance, and was therefore used for all subsequent experiments.

2.6.2 | Procedure

Eleven mice WT (5 female, 6 male) and 12 TG (6 female, 6 male) 2.5 months old were administered intraperitoneally a concentration of 50 mg/kg, placed in a sand wall transparent open field and video documented in video behavior of each animal for 60 minutes while taking a video with a web camera. Later on, recordings of each PTZ administration was analyzed off-line for determination of the four parameters described in the previous section (*latency, start, severity, and duration*).

2.7 | Statistical analysis

In patch-clamp experiments we defined a statistically stable period as a time interval (5–8 minutes) along which the mean amplitude of IPSC measured during any 1-minutes assessment did not vary according to an unpaired Student's *t* test. Miniature and spontaneous events were analyzed with the Clampfit software (pClamp 10, Molecular Devices/Axon, Foster City, CA), and MiniAnalysis (Synaptosoft, NJ, US). The minimum number of events considered per each condition was > 200 . In the analysis of miniature and spontaneous postsynaptic currents, only single events were considered for kinetic analysis. Detection threshold for miniature and spontaneous events was set at $\approx 150\%$ of the standard deviation of the noise (typical noise ≈ 4 –5 pA, threshold ≈ 7 –8 pA).

All data are expressed as mean \pm standard error of the mean. Pair pulse ratio (PPR) was calculated by dividing the mean of the second response by the mean the first response for each individual trace and then averaged (Atzori et al., 2005). Differences were assessed by comparing the same parameter with unpaired Student's *t* test. Data are reported as significantly different only if $p < 0.05$ (*).

3 | RESULTS

3.1 | Glutamatergic currents

We examined frequency, amplitude, rise-time, and decay-time of action potential-independent miniature excitatory synaptic currents (mEPSCs) in the presence of tetrodotoxin (TTX, 1 μ M) as well as of spontaneous excitatory synaptic currents (sEPSCs) in the absence of TTX. We found that the frequency of both mEPSCs and of sEPSCs was larger in TG vs. WT animals (representative traces in Figure 1A, B for mEPSCs, and in Figure 1G, H for sEPSCs, mean in Figure 1C, I for mEPSCs and sEPSCs, respectively). None of the other parameters measured significantly differed between TG and WT animals (mean mEPSC amplitude, rise-, and

decay-times in Figure 1D–F, for mEPSCs, and in Figure 1J–L, for sEPSC, respectively). These results suggest that TG animals may display a higher excitability.

3.2 | Inhibitory currents

We sought for possible differences between TG and WT animals in action potential-independent (miniature) inhibitory postsynaptic currents (mIPSCs, in TTX) and spontaneous inhibitory postsynaptic currents (sIPSCs). No differences were detected in mIPSC frequency, amplitude, rise-, or decay-time (representative traces in Figure 2A,B, mean frequency Figure 2C, mean amplitude Figure 2D, mean rise- and decay-times in Figure 2E, F). Likewise, no differences were present in sIPSC frequency, amplitude, rise-, or decay-time (representative traces in Figure 2G, H, mean frequency Figure 2I, mean amplitude Figure 2L, mean rise- and decay-times in Figure 2M, N).

In an attempt to determine possible differences between extrasynaptic tonic γ -amino butyric acid (GABA)-ergic currents we used a standard technique consisting in first enhancing with THIP (5 μ M) the currents mediated by GABA_ARs containing the δ subunit—peculiar of extrasynaptic GABA_ARs—and then blocking the enhanced tonic currents with the GABA_AR blocker picrotoxin (100 μ M) or bicuculline methiodide (20 μ M, Figure 2O) still in the presence of THIP. The tonic component of GABA_AR-mediated current (I_{tonic}) was calculated as THIP-induced increase in the holding current I_h (Figure 2O, mean in Figure 2P), and $I_{\text{tonic}} = I_h(\text{ctr}) - I_h(\text{PTX})$, the difference between the THIP-enhanced I_h and the I_h remaining after picrotoxin or bicuculline block (see Figure 2O, mean in Figure 2Q). No differences were detected between TG and WT in I_{tonic} ($n = 12$ WT and 14 TG, n.s.) or in the THIP-induced I_h enhancement. Statistical significance of the measurement was not affected by normalization of the current to neuronal surface (see the *Methods* section) for either measurement (Figure 2R, S, respectively).

3.3 | Evoked synaptic currents

The ratio between excitatory and inhibitory synaptic currents is an important parameter of neuronal sensitivity. By using a low Cl^- intracellular solution and recording glutamatergic currents mediated by amino-propionic acid receptors (AMPA) or GABA_ARs at two different holding potentials (see the *Methods* section), as in previous work (Garcia-Oscos et al., 2012), we were able to measure the excitatory-to-inhibitory synaptic ratio ($I_{\text{AMPA}}/I_{\text{GABA}}$) within the same cell (representative traces in Figure 3A, B, for WT and TG animals, respectively). No differences between WT and TG animals were found in $I_{\text{AMPA}}/I_{\text{GABA}}$ (mean $I_{\text{AMPA}}/I_{\text{GABA}} = 0.57 \pm 0.11$ in WT, vs. 0.60 ± 0.09 in TG animals, n.s., Figure 3C).

Besides an AMPAR-dependent component, most glutamatergic synapses possess a further component dependent on the activation of N-methyl D-aspartate receptors (I_{NMDA}). We calculated the ratio $I_{\text{AMPA}}/I_{\text{NMDA}}$ using a solution containing the GABA_AR blocker bicuculline (10 μ M) after measuring separately either component. I_{AMPA} was determined as a peak value of the evoked EPSC at $V_h = -65$ mV, while

glutamatergic synaptic activity

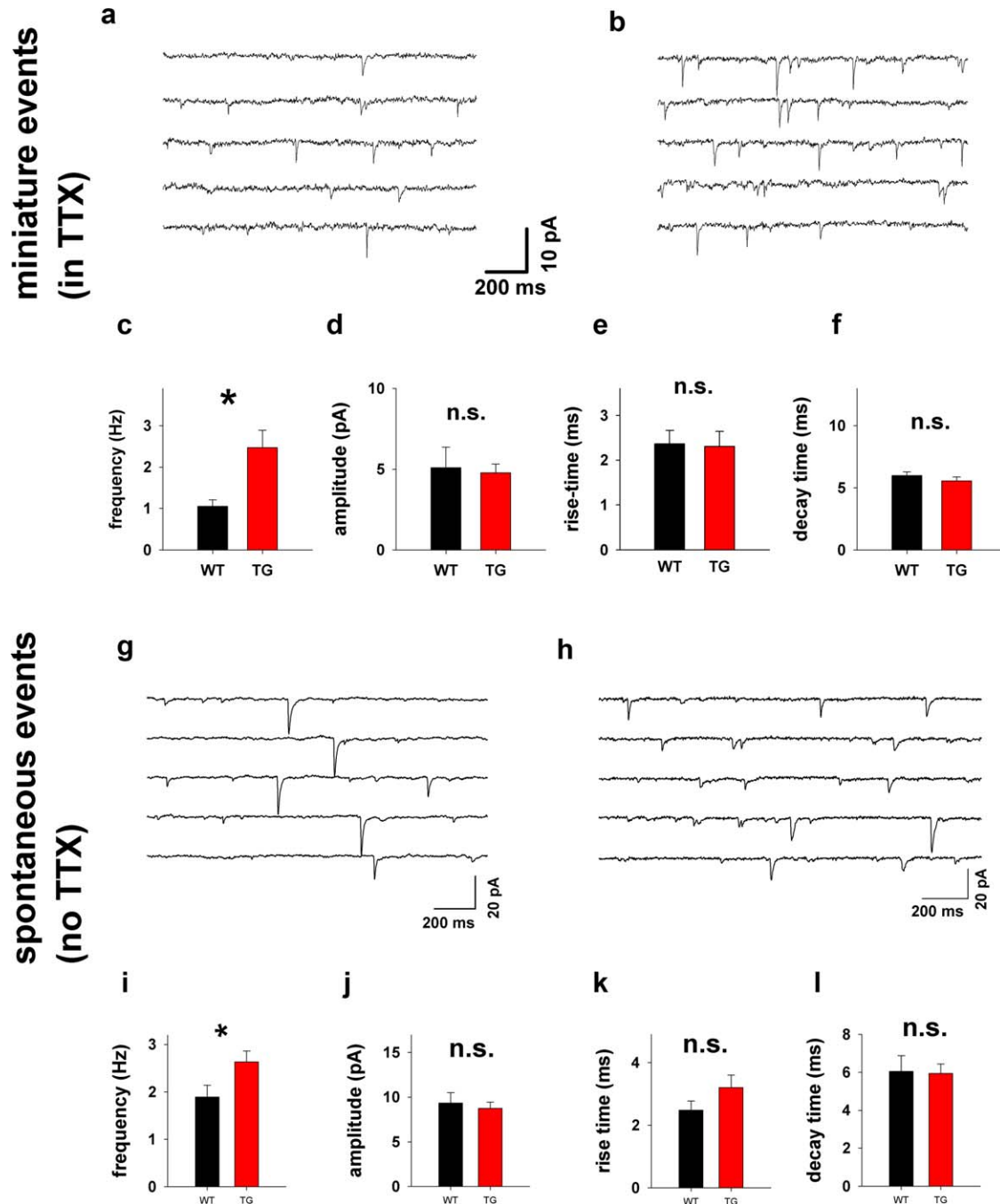


FIGURE 1 The absence of IL-6 trans-signaling increases glutamatergic synaptic frequency. (A and B) Representative traces of mEPSC in WT and TG animals, respectively. (C, D, E, and F) Bar graphs representing the mean \pm s.e.m. of the frequency, amplitude, rise- and decay-time of mEPSC, respectively. The asterisk (*) represents statistical significance, while n.s. indicates nonsignificant differences. (G and H) Representative traces of sEPSC in WT and TG animals, respectively. (I, J, K, and L) Bar graphs representing the mean \pm s.e.m. of the frequency, amplitude, rise- and decay-time of sEPSC, respectively. The asterisk (*) represents statistical significance, while n.s. indicates nonsignificant differences

339 I_{NMDA} was determined as the late current (95 ms past the stimulation
340 artifact) at a holding potential $V_h = +60$ mV in order to remove the
341 voltage-dependent Mg^{2+} block, similar to previous work (Dufour et al.,
342 2006) (representative traces are shown in Figure 3D, E for WT and TG
343 animals, respectively, for details see the Methods section). No differ-

ence between WT and TG animals was detected in $I_{\text{AMPA}}/I_{\text{NMDA}}$ 344
(mean: 5.8 ± 1.2 in WT vs. 5.8 ± 1.1 in TG animals, $n = 12$ and 15 , 345
respectively, n.s., Figure 3F). 346

The same recordings were used to calculate pair pulse ratio (PPR 347
with an interpulse delay of 200 ms), rise-time, and decay time for both 348

GABAergic currents

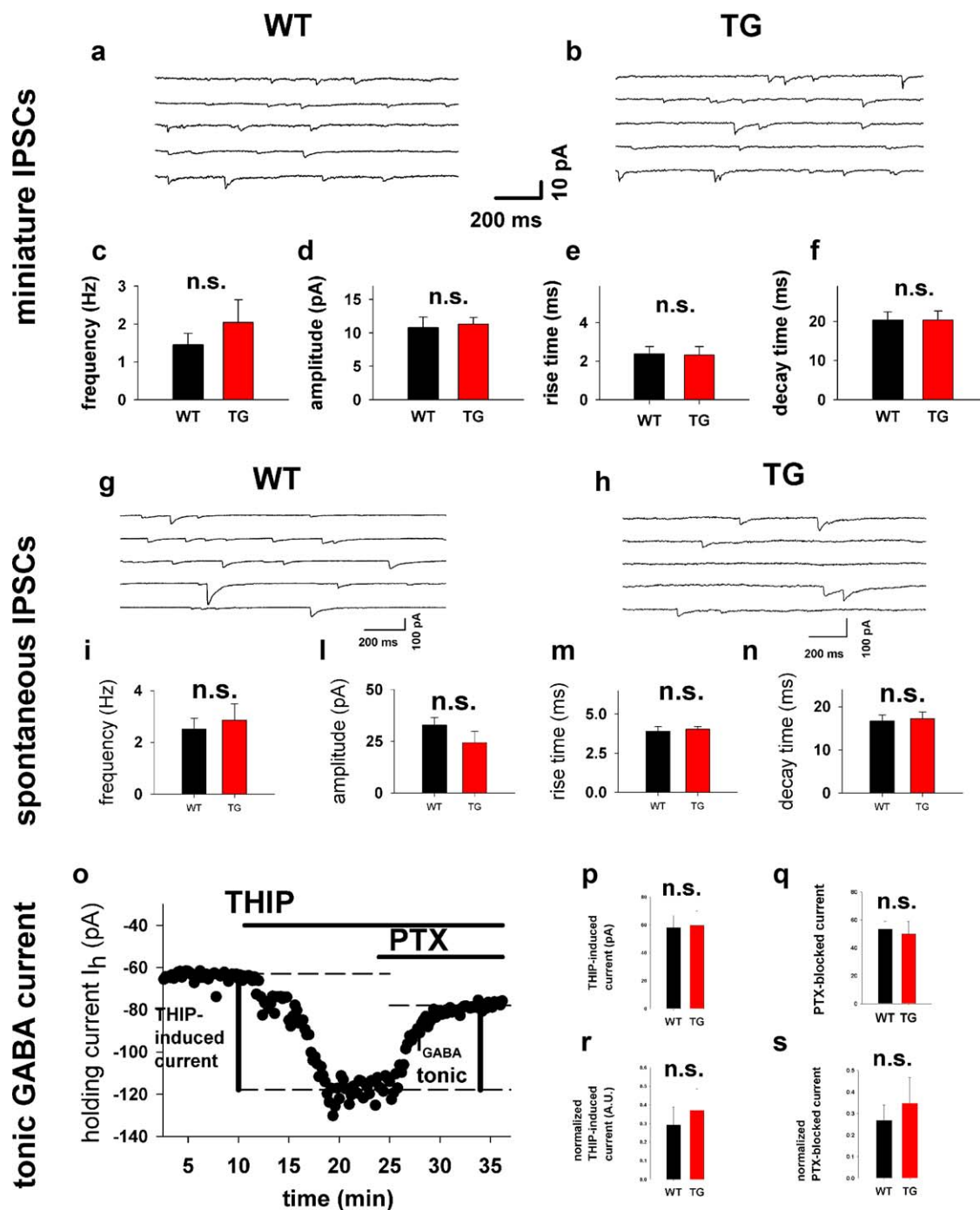


FIGURE 2 IL-6 trans-signaling does not affect inhibitory GABAergic currents. (A and B) Representative traces of mIPSC in WT and TG animals, respectively. (C, D, E, and F) Represent the mean \pm s.e.m. of mIPSC frequency, amplitude, rise-, or decay-time. No statistical differences were detected in any of these parameters. (G and H) Representative traces of sIPSC in WT and TG animals, respectively. (I, L, M, and N) Represent the mean \pm s.e.m. of sIPSC frequency, amplitude, rise-, or decay-time. No statistical differences were detected in any of these parameters. (O) Method for determining the amplitude of extrasynaptic GABA_AR-mediated current: each dot in the time-course graph represents the resting current (I_h), measured every 12 seconds in a V-clamp recording. Bath-application of gaboxadol (THIP, 5 μ M, a selective enhancer of the specific GABA_A δ subunit), increases I_h . A subsequent application of the GABA_AR blocker picrotoxin or bicuculline reduces I_h . Both the THIP-induced and the GABA_AR-blocker sensitive current (tonic I_{GABA}) were measured as shown in the example. P and Q: No differences were detected between WT and TG animals neither in the amplitude of the THIP-induced nor in tonic I_{GABA} . (R and S) The same data in B and C were normalized to the neuronal surface determined from neuronal decay time and input resistance measured with a 5 mV pulse delivered in each recording. No differences between TG and WT animals were detected even after current normalization

evoked PCSs

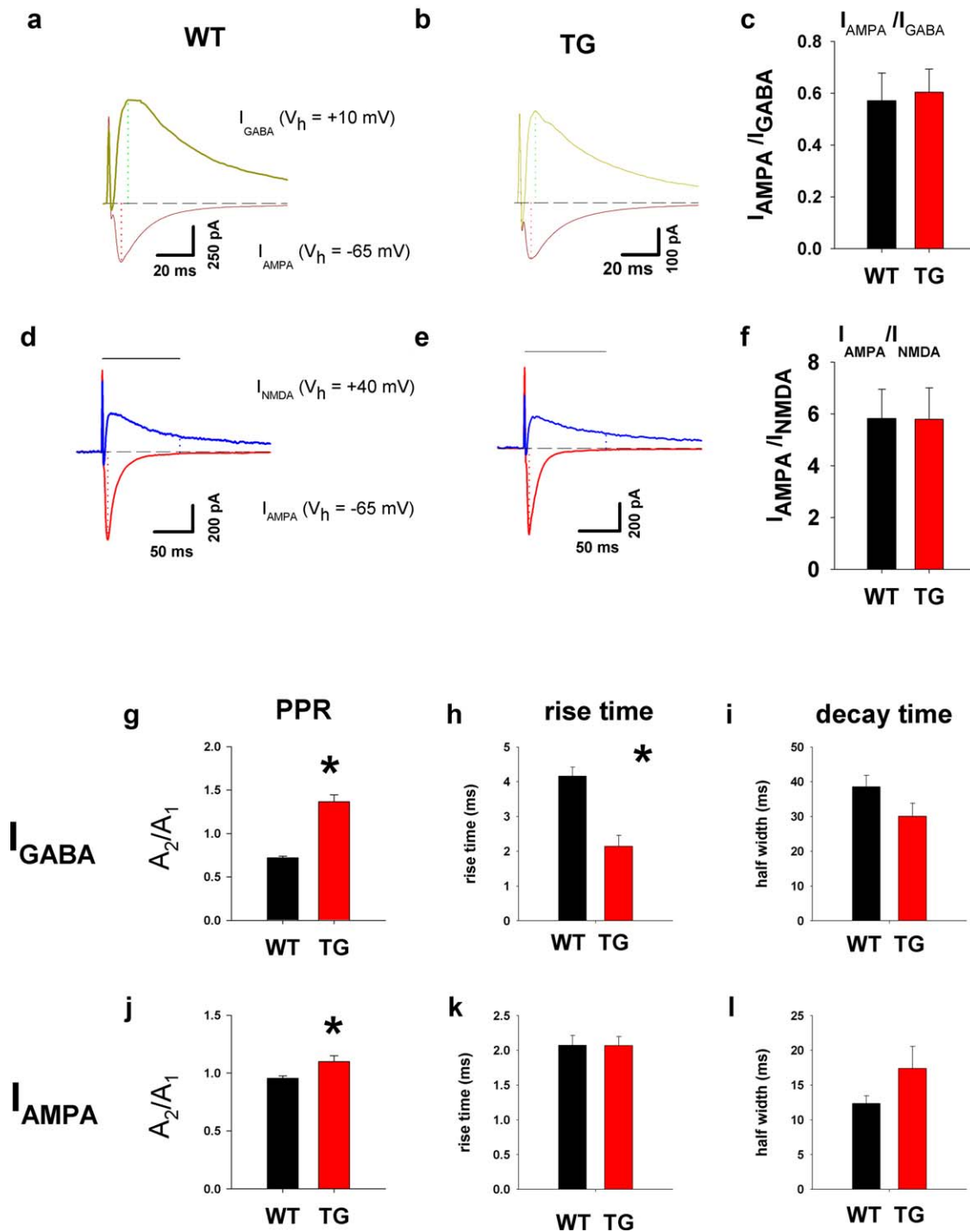


FIGURE 3 Effect of IL-6 trans-signaling on the ratio between electrically evoked synaptic currents and their kinetics. (A and B) Representative traces showing the GABA_A-mediated (I_{GABA} , green) and AMPAR-mediated (I_{AMPA} , brown) synaptic currents (measured in the same cell) in WT (A) and in TG (B) animals. (C) Ratio I_{AMPA}/I_{GABA} in WT (black bar) vs. TG animals (red bar). No significant differences were detected. (D and E) Representative traces showing the NMDAR-mediated (I_{NMDA} , blue) and AMPAR-mediated (I_{AMPA} , red) synaptic currents (measured in the same cell) in WT (A) and in TG (B) animals. (C) Ratio I_{AMPA}/I_{NMDA} in WT (black bar) vs. TG animals (red bar). No significant differences were detected. (G and H) rise- and decay times of eIPSC. TG animal's rise times are significantly shorter compared to WT ones. (I and J) Rise and decay times of eEPSC. No differences in eEPSC kinetic parameters were identified between TG and WT animals

TABLE 1 Summary of the synaptic properties of GFAP-sgp130Fc vs.WT C57BL/6 mice (TG vs.WT)

	GABAergic transmission	change	Glutamatergic transmission	change	ratios	change
mIPSC	amplitude	0	mEPSC	amplitude	0	$\frac{I_{AMPA}}{I_{GABA}}$
	frequency	0	frequency	↑	$\frac{I_{AMPA}}{I_{NMDA}}$	0
	rise time	0	rise time	0		
	decay time	0	decay time	0		
sIPSC	amplitude	0	sEPSC	amplitude	0	
	frequency	0	frequency	↑		
	rise time	0	rise time	0		
	decay time	0	decay time	0		
eIPSC	PPR	↑	eEPSC	PPR	↑	
	rise time	↓	rise time	0		
	decay time	0	decay time	0		
extrasynaptic	THIP-induc.	0				
	picrot.-sens.	0				

eIPSCs (mean in Figure 3G–I) and eEPSCs (mean in Figure 3J–L), respectively. TG animals displayed a larger PPR for both eIPSCs (0.72 ± 0.02 for WT, vs. 1.37 ± 0.08 for TG, $n = 12$ and 15 , respectively, $p < 0.05$) and eIPSCs (0.96 ± 0.02 for WT, vs. 1.1 ± 0.05 for TG, $n = 12$ and 15 , respectively, $p < 0.05$). Rise time of eIPSC was shorter in TG animals compared to WT (4.1 ± 0.3 for WT, vs. 2.2 ± 0.3 , $p < 0.05$), whereas all remaining kinetic parameters of electrically evoked PSCs did not change.

Altogether, the previous results indicate a series of differences between TG and WT mice, suggesting that transgenic animals may display a larger overall excitability. The results summarizing the differences in synaptic transmission between TG and WT are reported in

Table 1.

3.3.1 | Central IL-6 trans-signaling protects from PTZ-induced seizures

In order to determine possible differences in excitability threshold we compared the sensitivity to seizures in WT vs.TG animals. We used a convulsion model based on the intraperitoneal injections of the GABA_AR antagonist pentylenetetrazole (PTZ) to induce status epilepticus (Erdoğan, Gölgeli, Arman, & Ersoy, 2004) in the experimental animals. We compared TG and WT for the severity of the PTZ-induced seizures with the help of a semi-quantitative (Racine) scale evaluating seizure latency, gravity, and duration of the convulsive PTZ-induced episode (see the Methods section).

After a preliminary set of experiment in WT animals, in which the injection of 25 mg/kg of PTZ ($n = 3$) did not cause any effect, 50 mg/kg did induce measurable effects ($n = 3$), while injections of 75 mg/kg induced death ($n = 3$), we further refined the search of the optimal concentration to perform the final form of the experiments, by testing the effects of the doses of 40, 50, and 60 mg/kg on the characteristics of a

convulsive episode following the i.p. administration of PTZ. While *start*, *severity*, and *duration* of the epileptic events did not display significant differences among the three PTZ doses, the *latency* showed a clear trend toward shorter intervals ($n = 6$, data not shown), prompting at 50 mg/kg as the lowest dose eliciting a short-delay convulsion, concentration which was chosen for the next phase experiment.

The *latency* and *start* of the PTZ-induced events were not significantly different between WT and TG animals (Figure 4A, B), although a tendency to shorter intervals was present ($n = 10$ WT animals and $n = 11$ TG animals). On the contrary, the severity and duration of the PTZ-induced events were larger for TG animals (Figure 4C: 1.45 ± 0.22 arbitraryunits WT vs. 2.62 ± 0.47 a.u. TG; Figure 4D, 0.59 ± 0.27 minutes WT vs. 1.78 ± 0.84 minutes TG, same sample as Figure 4A, B).

4 | DISCUSSION

In previous work by us and others (Atzori et al., 2012; Kawasaki et al., 2008) it was found that acute administration of IL-6 reduces the amplitude of GABAergic synaptic currents, with scant or no effect on excitatory currents. Furthermore, we showed that LPS injections also decrease GABAergic signaling in an IL-6-dependent fashion, leading us to hypothesize that IL-6 plays a critical role in changes of the excitatory-to-inhibitory ratio brought about by stress. In the present investigation we aimed to identify differences in basal synaptic transmission between WT and the TG animals.

By comparing WT animals with genetically modified mice in which central IL-6 trans-signaling was blocked, we showed in this study for the first time that central IL-6 trans-signaling modulates basal synaptic transmission as well as seizure excitability.

The increase in both mEPSC and sEPSC frequency suggests that the presynaptic component of excitatory synapses undergo an

properties of PTZ-induced seizures

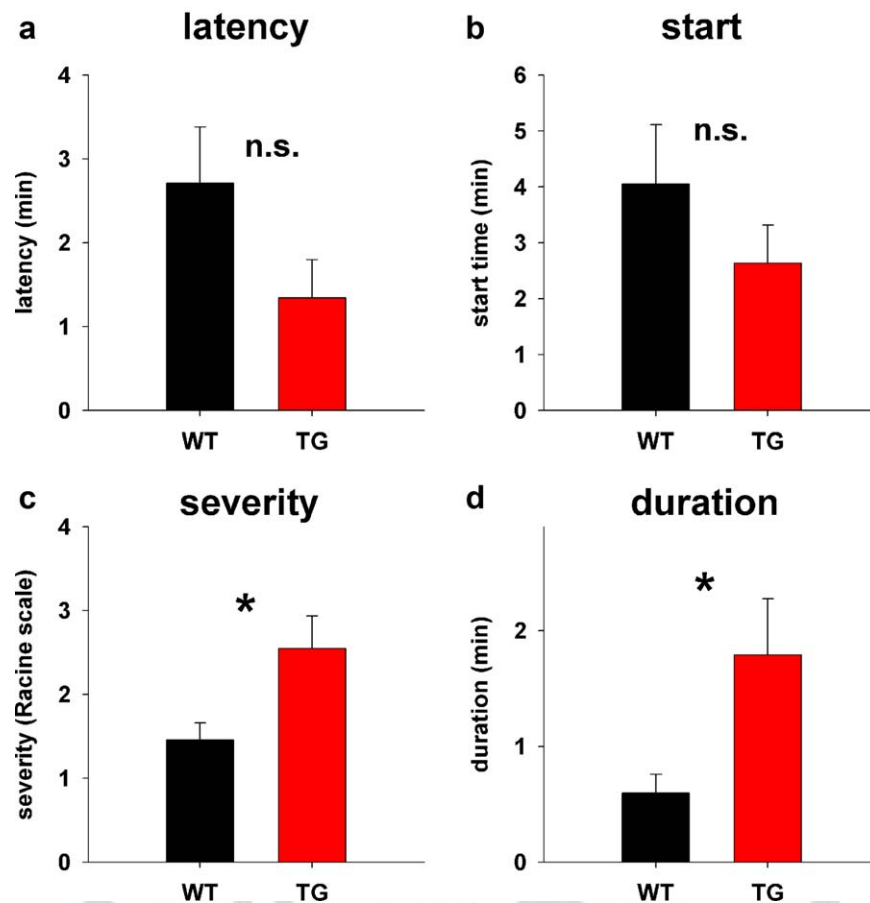


FIGURE 4 The absence of IL-6 trans-signaling worsens PTZ-induced seizures. (A) Convulsion beginning (*latency*), (B) time of the appearance of behavioral effects like mouth and facial contractions (*start*), (C) convulsion score in the Racine Scale (*severity*), (D) convulsion duration (*duration*) of the convulsive episode (PTZ at 50 mg/kg). TG mice do not display latencies or start time significantly different from WT animals after PTZ injections (Figure 2A, B), but do show increased severity (Figure 2C) and duration (Figure 2D) of the epileptic episode

enhanced development in TG vs. WT animals, possibly ending up with an enhanced presynaptic function or even with a larger number of excitatory synapses in the TG animal compared to the WT one. Given the postsynaptic nature of the negative effect of IL-6 on GABAergic transmission (Garcia-Oscos et al., 2012), and the increased postsynaptic GABAergic response observed previously in TG compared to WT animals (Garcia-Oscos et al., 2015)—further supported by the shorter rise-time in evoked IPSCs—we considered the possibility that IL-6 trans-signaling affected the basal levels of GABAergic currents. Yet, neither mIPSCs, sIPSC, nor THIP-sensitive or the picrotoxin-sensitive components of tonic GABAergic currents displayed any significant difference, before or after current normalization to cell surface area, suggesting that block of IL-6 trans-signaling during development does not alter basal synaptic inhibition.

Changes in pair pulse ratio of electrically evoked synaptic signals corroborate the hypothesis that IL-6 trans-signaling modulates action potential-dependent release in both excitatory and inhibitory synapses, possibly by affecting cellular conductances involved in the action potential.

We also considered the possibility that the ratio between synaptic excitation and inhibition, and/or the proportion between AMPAR- and NMDAR-mediated glutamatergic synaptic currents—two parameters critical for neuronal excitability and plasticity—were modulated by IL-6 trans-signaling. Measurement of either by standard methods (Dufour et al., 2006; Garcia-Oscos et al., 2012) did not reveal any significant difference in either parameter, suggesting that whichever synaptic change is associated with an absent IL-6 trans-signaling, both the synaptic balance between excitation and inhibition and the gross proportion between AMPAR- and NMDAR-mediated transmission is resettled to basal level, at least in the absence of any external challenge (stress).

The differences identified in the present work do not necessarily reflect or are caused by the absence of IL-6 trans-signaling and the consequent failure to mediate acute effects of stress on synaptic transmission (in TG animals). In fact, the differences that we detected may rather be caused by the (yet unknown) long-term effects of basal IL-6 trans-signaling on glutamatergic synaptic transmission associated with either modulation of GABAergic transmission (Garcia-Oscos et al., 2012), direct neurotrophic effects of IL-6 on the cortical (excitatory

and/or inhibitory) circuitry (Levin & Godukhin, 2017), or even by indirect, glia-mediated neurotrophic effects (Parish et al., 2002).

While the present electrophysiological results suggest that the absence of IL-6 trans-signaling during development—and possibly throughout the animal life—elicits mostly higher levels of spontaneous (action potential-independent as well as action potential-dependent) excitatory activity, without altering either the excitatory-inhibitory synaptic ratio nor the ratio between AMPAR-mediated and NMDAR-mediated signaling (calculated from single cell electrically evoked currents), it is not immediately obvious whether chronic IL-6 trans-signaling block would be associated with an altered overall excitability of the overall system. We chose to measure PTZ-induced seizure sensitivity because of the short latency of the Test (1–2 minutes), eliciting a response from an organism which did not have the time to undergo longer-term biochemical alterations, different from the LPS challenge, which occurs about 4 hours after intraperitoneal injections.

The increased sensitivity of TG animals to PTZ-induced seizures clearly indicates that TG animals are more excitable compared to WT ones, suggesting that IL-6 trans-signaling exerts an overall inhibitory effect on basal excitability. These data are in line with an enhanced basal excitability suggested by the increase EPSC frequency in the PFC recordings, corroborated by previous results (Benedict et al., 2009; Braun et al., 2013; Oyanedel et al., 2015), and are consistent with the anecdotal observation of increase excitability and aggression within and between TG animals.

Given that the IL-6/IL-6 R transducer gp130 belongs to the family of membrane tyrosine kinases similar to neuronal growth factor which includes nerve growth factor (NGF), neurotrophin 3 and 4 (NT3 and NT4) and BDNF, it is remarkable that an impaired or absent IL-6 trans-signaling affected excitatory synapses in a similar way to BDNF (Wu et al., 2004), while at the same time enhancing also inhibitory transmission (Bardoni, Ghiri, Salio, Prandini, & Merighi, 2007), tempting the speculation that IL-6 and BDNF may play complementary roles in the development and/or synaptic stabilization of inhibitory synapses.

5 | CONCLUSIONS

The present work suggests that IL-6 trans-signaling does modulate basal excitatory as well as—to a lesser extent—inhibitory synaptic transmission. While the changes in mIPSC rise-time, together with the increased level of I/O eIPSC currents (Garcia-Oscos et al., 2015) suggest the influence of IL-6 trans-signaling on a postsynaptic component of inhibitory synaptic transmission, in agreement with a working hypothesis formulated previously (Atzori et al., 2012; Garcia-Oscos et al., 2012), the change in eIPSC PPR may indicate an additional presynaptic component, not necessarily associated with intrasynaptic mechanisms of GABA release, but rather with a modulation of action-potential dependent GABAergic interneurons or other cellular mechanisms.

Further work will be necessary to assess the role of IL-6 trans-signaling in stress-induced plasticity of neuronal synaptic networks. A special care should be used to extrapolate long- from short-term effects of

IL-6, given that different temporal patterns of cytokine release associated parallel physiological, emotional, or cognitive stressors may bring about different—possibly opposite (adaptive or maladaptive)—response to stress.

AUTHORS CONTRIBUTION

RCO, EER, FGO, MMM, and HS performed electrophysiology experiments and corresponding analysis, JVM, prepared the animals and performed and analyzed the behavioral experiments, SRJ was responsible for the molecular biology and preparation of the transgenic animals, MA wrote the manuscript. All the authors contributed to experiment planning, discussion of the results, and approval of the manuscript.

ACKNOWLEDGMENTS

The work has been conducted with funds from CONACyT (CB-2013-01 221653) and PROMEP 2014 to M.A. None of the authors has any conflict of interest related to this material.

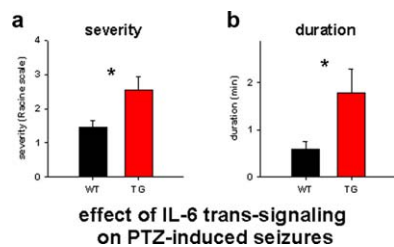
REFERENCES

- Atzori, M., Garcia-Oscos, F., & Mendez, J. A. (2012). Role of IL-6 in the etiology of hyperexcitable neuropsychiatric conditions: experimental evidence and therapeutic implications. *Future Medicinal Chemistry*, 4, 2177–2192.
- Atzori, M., Kanold, P. O., Pineda, J. C., Flores-Hernandez, J., & Paz, R. D. (2005). Dopamine prevents muscarinic-induced decrease of glutamate release in the auditory cortex. *Neuroscience*, 134, 1153–1165.
- Banerjee, A., Garcia-Oscos, F., Roychowdhury, S., Galindo, L. C., Hall, S., Kilgard, M. P., & Atzori, M. (2013). Impairment of cortical GABAergic synaptic transmission in an environmental rat model of autism. *The International Journal of Neuropsychopharmacology*, 16, 1309–1318.
- Bardoni, R., Ghiri, A., Salio, C., Prandini, M., & Merighi, A. (2007). BDNF-mediated modulation of GABA and glycine release in dorsal horn lamina II from postnatal rats. *Developmental Neurobiology*, 67, 960–975.
- Behrens, M. M., Ali, S. S., & Dugan, L. L. (2008). Interleukin-6 mediates the increase in NADPH-oxidase in the ketamine model of schizophrenia. *The Journal of Neuroscience*, 28, 13957–13966.
- Belem da Silva, C. T., Costa M de, A., Bortoluzzi, A., Pfaffenseller, B., Vedana, F., Kapczinski, F., & Manfro, G. G. (2016). Cytokine Levels in Panic Disorder. *Psychosomatic Medicine*, 79, 1.
- Benedict, C., Scheller, J., Rose-John, S., Born, J., & Marshall, L. (2009). Enhancing influence of intranasal interleukin-6 on slow-wave activity and memory consolidation during sleep. *FASEB Journal*, 23, 3629–3636.
- Braun, O., Dewitz, C., Moller-Hackbarth, K., Scheller, J., Schiffelholz, T., Baier, P. C., & Rose-John, S. (2013). Effects of blockade of peripheral interleukin-6 trans-signaling on hippocampus-dependent and independent memory in mice. *Journal of Interferon & Cytokine Research*, 33, 254–260.
- Campbell, I. L., Abraham, C. R., Masliah, E., Kemper, P., Inglis, J. D., Oldstone, M. B., & Mucke, L. (1993). Neurologic disease induced in transgenic mice by cerebral overexpression of interleukin 6. *Proceedings of the National Academy of Sciences of the United States of America*, 90, 10061–10065.

- 548 Campbell, I. L., Erta, M., Lim, S. L., Frausto, R., May, U., Rose-John, S., ...
549 Hidalgo, J. (2014). Trans-signaling is a dominant mechanism for the
550 pathogenic actions of interleukin-6 in the brain. *The Journal of Neuro-*
551 *science*, 34, 2503–2513.
- 552 Chalaris, A., Garbers, C., Rabe, B., Rose-John, S., & Scheller, J. (2011).
553 The soluble Interleukin 6 receptor: generation and role in inflamma-
554 tion and cancer. *European Journal of Cell Biology*, 90, 484–494.
- 555 Drasbek, K. R., & Jensen, K. (2006). THIP, a hypnotic and antinociceptive
556 drug, enhances an extrasynaptic GABAA receptor-mediated conduct-
557 ance in mouse neocortex. *Cerebral Cortex (New York, N.Y. : 1991)*, 16,
558 1134–1141.
- 559 Dufour, F., Liu, Q. Y., Gusev, P., Alkon, D., & Atzori, M. (2006). Choles-
560 terol-enriched diet affects spatial learning and synaptic function in
561 hippocampal synapses. *Brain Research*, 1103, 88–98.
- 562 Erdoğan, F., Gölgeli, A., Arman, F., & Ersoy, A. O. (2004). The effects of
563 pentylenetetrazole-induced status epilepticus on behavior, emotional
564 memory, and learning in rats. *Epilepsy & Behavior*, 5, 388–393.
- 565 Garcia-Oscos, F., Peña, D., Housini, M., Cheng, D., Lopez, D., Borland,
566 M. S., ... Atzori, M. (2015). Vagal nerve stimulation blocks interleukin
567 6-dependent synaptic hyperexcitability induced by lipopolysaccharide-
568 induced acute stress in the rodent prefrontal cortex. *Brain, Behavior, and*
569 *Immunity*, 43, 149–158.
- 570 Garcia-Oscos, F., Salgado, H., Hall, S., Thomas, F., Farmer, G. E., Bermeo,
571 J., ... Atzori, M. (2012). The stress-induced cytokine interleukin-6
572 decreases the inhibition/excitation ratio in the rat temporal cortex
573 via trans-signaling. *Biological Psychiatry*, 71, 574–582.
- 574 Getova, D. P., & Mihaylova, A. S. (2011). A study of the effects of lamo-
575 trigine on mice using two convulsive tests. *Folia Medica*, 53, 57–62.
- 576 Holmes, A., & Wellman, C. L. (2009). Stress-induced prefrontal reorgan-
577 ization and executive dysfunction in rodents. *Neurosci Neuroscience*
578 *and Biobehavioral Reviews*, 33, 773–783.
- 579 Kawasaki, Y., Zhang, L., Cheng, J. K., & Ji, R. R. (2008). Cytokine mecha-
580 nisms of central sensitization: distinct and overlapping role of
581 interleukin-1 β , interleukin-6, and tumor necrosis factor- α in
582 regulating synaptic and neuronal activity in the superficial spinal
583 cord. *The Journal of Neuroscience*, 28, 5189–5194.
- 584 Lehtimäki, K. A., Liimatainen, S., Peltola, J., & Arvio, M. (2011). The
585 serum level of interleukin-6 in patients with intellectual disability and
586 refractory epilepsy. *Epilepsy Research*, 95, 184–187.
- 587 Levin, S. G., & Godukhin, O. V. (2017). Modulating effect of cytokines on
588 mechanisms of synaptic plasticity in the brain. *Biochemistry*, 82, 264–
589 274.
- 590 Li, G., Bauer, S., Nowak, M., Norwood, B., Tackenberg, B., Rosenow, F.,
591 ... Hamer, H. M. (2011). Cytokines and epilepsy. *Seizure*, 20, 249–
592 256.
- 593 Monje, F. J., Cabatic, M., Divisch, I., Kim, E. J., Herkner, K. R., Binder, B.
594 R., & Pollak, D. D. (2011). Constant darkness induces IL-6-dependent
640 depression-like behavior through the NF- κ B signaling pathway. *595*
The Journal of Neuroscience, 31, 9075–9083. *596*
- Nowell, M. A., Williams, A. S., Carty, S. A., Scheller, J., Hayes, A. J., Jones,
597 G. W., ... Jones, S. A. (2009). Therapeutic targeting of IL-6 trans sig-
598 naling counteracts STAT3 control of experimental inflammatory
599 arthritis. *Journal of Immunology (Baltimore, Md 1950)*, 182, 613–622. *600*
- Oyanedel, C. N., Kelemen, E., Scheller, J., Born, J., & Rose-John, S. *601*
(2015). Peripheral and central blockade of interleukin-6 trans-signal-
602 ing differentially affects sleep architecture. *Brain, Behavior, and Immu-*
603 *nity*, 50, 178–185. *604*
- Parish, C. L., Finkelstein, D. I., Tripanichkul, W., Satoskar, A. R., Drago, J.,
605 & Horne, M. K. (2002). The role of interleukin-1, interleukin-6, and
606 glia in inducing growth of neuronal terminal arbors in mice. *The Jour-*
607 *nal of Neuroscience*, 22, 8034–8041. *608*
- Rabe, B., Chalaris, A., May, U., Waetzig, G. H., Seegert, D., Williams, *609*
A. S., ... Scheller, J. (2008). Transgenic blockade of interleukin 6
610 transsignaling abrogates inflammation. *Blood*, 111, 1021–1028. *611*
- Rose-John, S. (2012). IL-6 trans-signaling via the soluble IL-6 receptor: *612*
importance for the pro-inflammatory activities of IL-6. *International*
613 *Journal of Biological Sciences*, 8, 1237–1247. *614*
- Roychowdhury, S., Zwierchowski, A. N., Garcia-Oscos, F., Olguin, R. C., *615*
Delgado, R. S., & Atzori, M. (2014). Layer- and area-specificity of the
616 adrenergic modulation of synaptic transmission in the rat neocortex. *617*
Neurochemical Research, 39, 2377–2384. *618*
- Sukoff Rizzo, S. J., Neal, S. J., Hughes, Z. A., Beyna, M., Rosenzweig-Lip-
619 son, S., Moss, S. J., & Brandon, N. J. (2012). Evidence for sustained
620 elevation of IL-6 in the CNS as a key contributor of depressive-like
621 phenotypes. *Translational Psychiatry*, 2, e199. *622*
- Waetzig, G. H., & Rose-John, S. (2012). Hitting a complex target: an *623*
update on interleukin-6 trans-signalling. *Expert Opinion on Therapeutic*
624 *Targets*, 16, 225–236. *625*
- Wolf, J., Rose-John, S., & Garbers, C. (2014). Interleukin-6 and its recep-
626 tors: A highly regulated and dynamic system. *Cytokine*, 70, 11–20. *627*
- Wu, K., Len, G., McAuliffe, G., Ma, C., Tai, J. P., Xu, F., & Black, I. B. *628*
(2004). Brain-derived neurotrophic factor acutely enhances tyrosine
629 phosphorylation of the AMPA receptor subunit GluR1 via NMDA
630 receptor-dependent mechanisms. *Molecular Brain Research*, 130, 178–
631 186. *632*

How to cite this article: Cuevas-Olguin R, Esquivel-Rendon E, *634*
Vargas-Mireles J, et al. Interleukin 6 trans-signaling regulates *635*
basal synaptic transmission and sensitivity to pentylenetetrazole- *636*
induced seizures in mice. *Synapse*. 2017;00:e21984. <https://doi.org/10.1002/syn.21984> *637*
638
639

SGML and CITI Use Only DO NOT PRINT



Inflammation does not only affect immune processes but also brain function, in an unknown manner. The proinflammatory cytokine interleukin-6 acts in the brain mainly through a mechanism denominated trans-signaling. Synaptic and behavioral excitability were increased in a transgenic model lacking interleukin 6 trans-signaling specifically in the brain.

WILEY
Author Proof

AUTHOR QUERY FORM

Dear Author,

During the preparation of your manuscript for publication, the questions listed below have arisen. Please attend to these matters and return this form with your proof.

Many thanks for your assistance.

Query References	Query	Remarks
AQ1	Citation of Garcia-Oscos et al., 2014 has been changed to Garcia-Oscos et al., 2015 as per the reference list. Please confirm	
AQ2	Kindly confirm the year of the reference Getova & Mihaylova, 2011.	
AQ3	Please confirm that given names (red) and surnames/family names (green) have been identified correctly.	

WILEY
Author Proof